nature genetics

Genome-wide maps of recombination and chromosome segregation in human oocytes and embryos show selection for maternal recombination rates

Christian S Ottolini[1,2,8], Louise J Newnham[3,8], Antonio Capalbo[4,8], Senthilkumar A Natesan[5], Hrishikesh A Joshi[5], Danilo Cimadomo[4], Darren K Griffin[2], Karen Sage[1], Michael C Summers[1,2], Alan R Thornhill[5], Elizabeth Housworth[6], Alex D Herbert[3], Laura Rienzi[4], Filippo M Ubaldi[4], Alan H Handyside[1,2,5,7] & Eva R Hoffmann[3]

Crossover recombination reshuffles genes and prevents errors in segregation that lead to extra or missing chromosomes (aneuploidy) in human eggs, a major cause of pregnancy failure and congenital disorders. Here we generate genome-wide maps of crossovers and chromosome segregation patterns by recovering all three products of single female meioses. Genotyping >4 million informative SNPs from 23 complete meioses allowed us to map 2,032 maternal and 1,342 paternal crossovers and to infer the segregation patterns of 529 chromosome pairs. We uncover a new reverse chromosome segregation pattern in which both homologs separate their sister chromatids at meiosis I; detect selection for higher recombination rates in the female germ line by the elimination of aneuploid embryos; and report chromosomal drive against non-recombinant chromatids at meiosis II. Collectively, our findings show that recombination not only affects homolog segregation at meiosis I but also the fate of sister chromatids at meiosis II.

Errors in chromosome segregation during the meiotic divisions in human female meiosis are a major cause of aneuploid conceptions, leading to implantation failure, pregnancy loss and congenital disorders[1]. The incidence of human trisomies increases exponentially in women from ~35 years of age, but, despite conservative estimates that 10–30% of natural conceptions are aneuploid[2], the underlying causes and their relative contributions are still unclear. In addition to maternal age, one important factor that predisposes to missegregation in both sexes is altered recombination. Recombinant chromosomes in offspring are the result of crossovers—the reciprocal exchange of DNA between homologous chromosomes (homologs). Together with sister chromatid cohesion, crossovers physically link the homolog pair together during the prophase stage of meiosis (**Fig. 1a**), which takes place during fetal development in females. The linkages have to be maintained for decades, as the two rounds of chromosome segregation only occur in adult women. By following the pattern of genetic markers such as SNPs on the two chromosomes inherited from the mother in trisomic conceptions, it has been inferred that some crossovers occur too close to centromeres[1,3–6], where they may disrupt the cohesion between the two sister chromatids[7,8]. Other crossovers have been suggested to be too far from the centromeres to mediate correct attachment or to be lacking altogether (non-exchange, E_0)[1,3–6]. If these inferences are correct, it follows that events that shape the recombination landscape in oocytes during fetal development affect the risk of women having an aneuploid conception decades later in adult life.

A limitation of these extensive population-based studies, however, is that only one of the products of meiosis is analyzed (the oocyte). This prevents direct identification of the origin of chromosome segregation errors and provides only partial information on the crossovers during prophase of meiosis I. The 'missing data' problem is so significant that even the meiotic origin of age-related trisomies has been challenged recently[9]. Another confounding factor is that the spontaneous miscarriages still births and affected live births on which our current knowledge is based represent only a minor fraction of the aneuploid embryos at conception. The majority of affected embryos are lost throughout pregnancy, resulting in substantial preclinical and clinical losses[2]. Thus, to understand the origin of human aneuploidies, it is necessary to assess all three meiotic products in unselected oocytes and embryos.

RESULTS

MeioMaps of single meioses in oocytes and embryos

To follow genome-wide recombination and chromosome segregation simultaneously, we recovered all three products of female meiosis, which include the first and second polar bodies (PB1 and PB2) and the

[1]The Bridge Centre, London, UK. [2]School of Biosciences, University of Kent, Canterbury, UK. [3]Genome Damage and Stability Centre, School of Life Sciences, University of Sussex, Brighton, UK. [4]GENERA (Gynecology, Endocrinology and Assisted Reproduction), Centers for Reproductive Medicine, Rome, Italy. [5]Illumina, Inc., Fulbourn, UK. [6]Department of Mathematics and Statistics, University of Indiana, Bloomington, Indiana, USA. [7]Institute of Integrative and Comparative Biology, University of Leeds, Leeds, UK. [8]These authors contributed equally to this work. Correspondence should be addressed to E.R.H. (eh58@sussex.ac.uk) or A.H.H. (ahandyside@illumina.com).

Received 11 November 2014; accepted 23 April 2015; published online 18 May 2015; doi:10.1038/ng.3306

corresponding activated oocytes or fertilized embryos (**Fig. 1**). We refer to these as oocyte-PB or embryo-PB trios (**Fig. 1a–c**). Ten embryo-PB trios were obtained after fertilization of the oocyte by intracytoplasmic sperm injection (ICSI). The embryos reached various stages of preimplantation development and originated from a single donor having preimplantation genetic screening (PGS) for recurrent miscarriage and who consented to follow-up genetic analysis of her embryos (**Fig. 1a** and **Supplementary Table 1**). A further 13 trios were generated without fertilization by activating mature, meiosis II–arrested oocytes with a calcium ionophore, which induced completion of meiosis II and extrusion of the PB2 (**Fig. 1b,c**). This method was highly successful (85%, $n = 40$; **Supplementary Table 2**) and did not alter the rate of meiosis II errors in the activated oocytes as compared to embryos generated by ICSI (6 of 299 versus 4 of 230; **Table 1**). The oocyte-PB

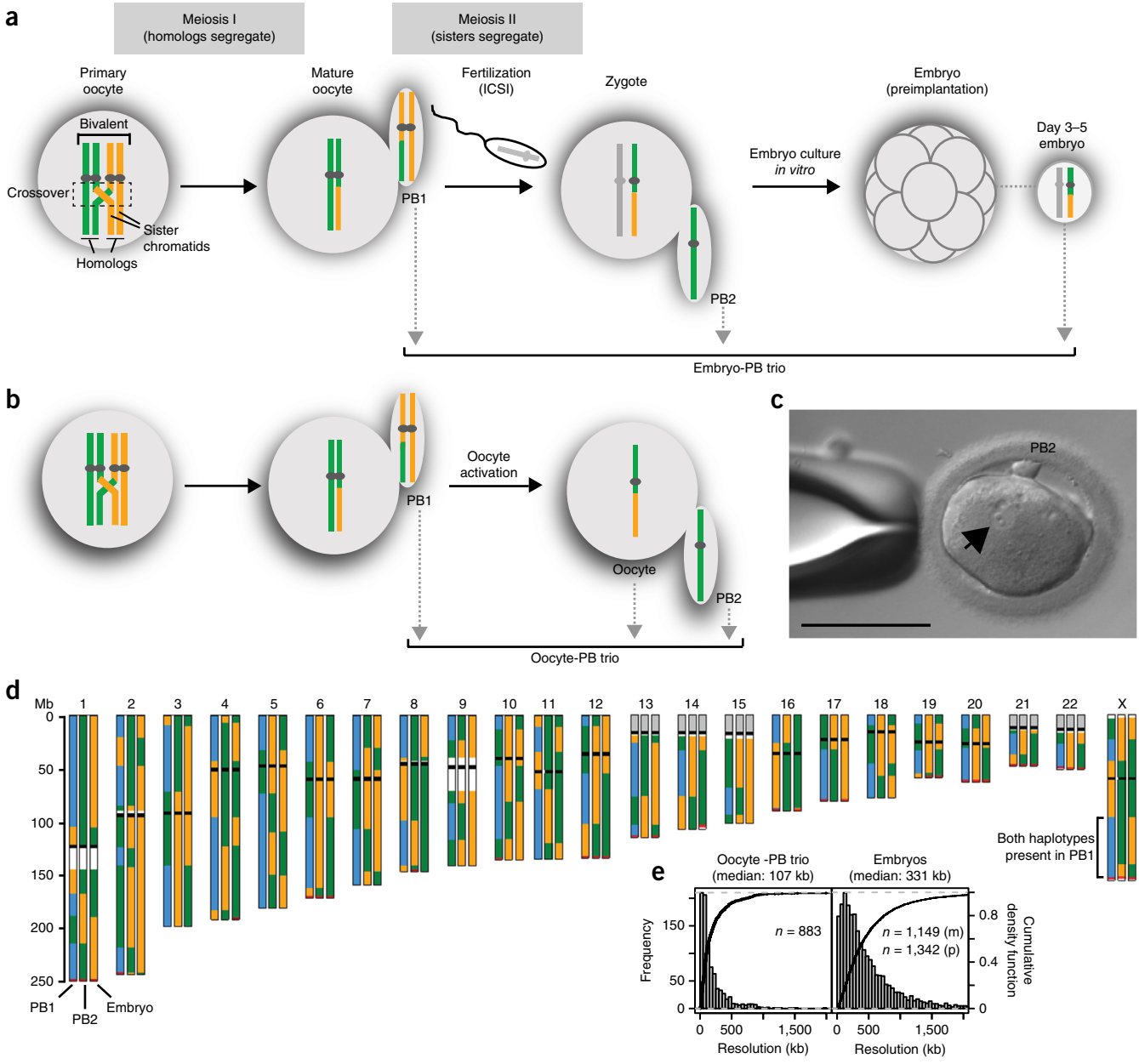

Figure 1 Human MeioMaps from embryos and oocytes together with their corresponding polar bodies. (**a**,**b**) The genotypes of the two maternal chromosomes are represented by green and orange. Crossovers, shown in the dashed box, occur during fetal development. The two polar bodies were sequentially biopsied (gray dotted arrows) to avoid misidentification. Maternal MeioMaps were deduced from the embryo following ICSI (**a**) or were directly assessed in the haploid oocyte after artificial activation (**b**). (**c**) An activated oocyte with a single pronucleus (arrow) and PB2. Scale bar, 110 µm. (**d**) An example of a MeioMap after genome-wide SNP detection and phasing (Online Methods). Each chromosome is represented by three vertical columns representing the three cells of the trio (PB1, PB2 and embryo or oocyte). The two phased maternal haplotypes are represented by green and orange. Blue represents the detection of both haplotypes. Regions where SNPs are not available on the array are shown in white (repetitive sequences on chromosomes 1 and 9) or gray (rDNA). Black bars illustrate the positions of the centromeres. Red bars show the last informative SNPs to call. Crossovers are manifested as reciprocal breakpoints in haplotypes (green to orange, blue to green, etc.) in two of the three cells. Note that the colors of the haplotype blocks across different chromosomes do not necessarily correspond to the same grandparent. (**e**) Histograms of the resolution of the crossovers. The resolution was 352 kb and 311 kb for maternal (m) and paternal (p) crossovers in the embryos, respectively.

Table 1 Origin and incidence of maternal aneuploidies.

Data set	Mean maternal age[a]	n[b]	Aneuploid oocytes (%)	Chromosome missegregation events[d]						Total chromosomes
				All events	Aneuploid outcome in oocyte	Gain in oocyte		Loss in oocyte		
						MI	MII	MI	MII	
Oocyte-PB trios	37.3 (33–41)	13	62	26	12	2	4	4	2	299
Embryo-PB trios	38.3	10	70	19	8	4	1	0	3	230
Embryo only	37.1 (34–42)	29[c]	54	ND	19	5	4	ND	ND	667

[a]Mean maternal age and range (in years). [b]Number of trios or embryos analyzed. [c]Twenty-eight embryos and one chorionic villus sample. [d]Statistical test for significance of meiosis II nondisjunction rates in oocyte-PB and embryo-PB trios: 6 of 299 in comparison to 4 of 230; G test with Williams' correction, $P = 0.82$.
ND, not determined as there was no information from polar bodies; MI, meiosis I; MII, meiosis II.

trios were obtained from five healthy female donors who had cryopreserved unfertilized eggs in the course of fertility treatment. Four of the five donors had achieved a pregnancy and live birth following *in vitro* fertilization (IVF), and all five consented to their remaining eggs being activated and undergoing genome analyses. The principle of isolating all three meiotic products is similar to the approach of using the polar bodies and recovering the female pronucleus from zygotes[10].

The trio data sets were complemented with data on recombination and aneuploidy rates from 29 embryos (without polar bodies) in which SNP genotyping and karyomapping[11] had previously been used for preimplantation genetic diagnosis (PGD). Because informative SNPs were available from both the mother and father, we were able to compare recombination events on paternal and maternal chromosomes and their associations with aneuploidy in embryos (**Supplementary Table 3**).

All samples underwent whole-genome amplification and were genotyped at ~300,000 SNP loci across the genome[11]. Across the 23 complete trios (meioses), we detected >4 million informative SNPs at high stringency, with an average resolution of 30 kb. The SNPs spanned >92% of the genome. For the oocyte-PB trios, genomic DNA from each donor was also genotyped to identify informative heterozygous SNP loci. For these trios, all heterozygous SNPs in the mother's genomic DNA are informative, whereas, in embryos, maternal and paternal heterozygous SNPs may be shared. Hence, the pattern of recombination for the paternal chromosomes was analyzed by karyomapping[11,12], and only the two subsets of SNP loci that were heterozygous in the father and homozygous in the mother (and vice versa) were identified and used to phase the two haplotypes from the given parent in the embryo[11,12]. The informative SNPs were phased using 'siblings' (ref. 10) that contained only a single chromatid from the mother (PB2, oocyte or maternal chromatid in embryo) or father (embryo). The reference (also known as the 'assumed ancestor')[10] was used to infer the crossover positions in the assumed offspring (that is, trios from the same parent; **Supplementary Fig. 1**). Crossovers at the same position in the 'assumed offspring' are highly unlikely to occur, and common crossovers can therefore be used to reform the reference genome, from which the two haplotypes can be deduced (**Supplementary Fig. 1**). Because many of our samples were single cells, we validated our workflow by comparing the recombination maps in 15 individual cells from a donor cell line to the recombination map obtained from genomic DNA and by assessing 10 individual blastomeres from the same embryo for direct comparison. In all cases, the concordance of frequencies for recombination events and their positions was >99%.

A typical MeioMap from a normal embryo-PB trio is shown in **Figure 1d**. MeioMaps show mendelian segregation of sequence polymorphisms (green and orange segregate 2:2 across haplotype regions) and independent assortment of different chromosomes in meiosis I (pericentromeric SNPs are used as a chromosome's fingerprint). Crossovers, which result in recombinant chromosomes, are evident by transitions between the two maternal haplotypes in the PB2 and oocyte or between a single maternal haplotype and heterozygous regions (PB1). We detected 39 cases of aneuploidy by the presence of informative SNPs for both maternal haplotypes in the pericentromeric and/or distal regions of chromosome arms or by the complete absence of informative SNPs for both maternal haplotypes for the entire chromosome (**Table 1**). Inferred chromosomal aneuploidies could be observed by array comparative genomic hybridization (aCGH; **Supplementary Fig. 2**). We also detected three gross structural rearrangements to chromosomes. Because two of the three meiotic products were affected (reciprocal gain and loss), this finding rules out the possibility that these rearrangements occurred during germline development and demonstrates that such rearrangements can occur during meiosis (**Supplementary Table 4**). Aneuploidy rates and the contribution of meiosis I and meiosis II errors were similar to those expected for this age range (33–41 years; **Table 1**)[13–17].

All gains and losses were reciprocal and involved two meiotic products, such that a gain of a chromosome in the oocyte was matched by loss of the chromosome in the PB1 or PB2. Of the 529 chromosome pairs assessed in the trios, we did not detect any deviation from the 4 chromatids expected to participate in meiosis. These observations firmly establish meiotic errors as the main contributor of aneuploid conceptions and do not support germline mosaicism in chromosome number before meiosis[9] as a major factor in the maternal age–related increase in human trisomies.

A new, reverse segregation pattern in human meiosis

To understand the nature of missegregation, we inferred chromosome segregation from the trios by following the informative SNPs at the pericentromere. Trisomies that occur at a high rate in the natural population of women of advanced maternal age[4] were originally hypothesized to arise by meiosis I nondisjunction, where both homologs segregate to the oocyte at meiosis I, followed by a normal second division[18] (**Fig. 2a** and **Supplementary Fig. 3a**). However, cytological examination of human oocytes that failed to fertilize in IVF clinics suggested that precocious separation of sister chromatids (PSSC) was the major cause of human age-related trisomies[19], at least in a clinical setting (**Fig. 2a** and **Supplementary Fig. 3b**). Having the genetic identity of the chromatids not only from the embryos or oocytes but also from their matched polar bodies allows the two segregation patterns to be distinguished, as the chromosome signatures in the two polar bodies will differ (**Fig. 2a**). Confirming previous studies using aCGH for copy number analysis in trios[20], classical meiosis I nondisjunction was relatively rare and PSSC was more frequent, at least in hormone-stimulated IVF-treated patients (**Fig. 2a–c**). The preponderance of PSSC in comparison to meiosis I nondisjunction is consistent with findings in oocytes from younger Chinese donors, although aneuploidy rates were much lower in that age group (25–35 years; **Fig. 2b**)[10].

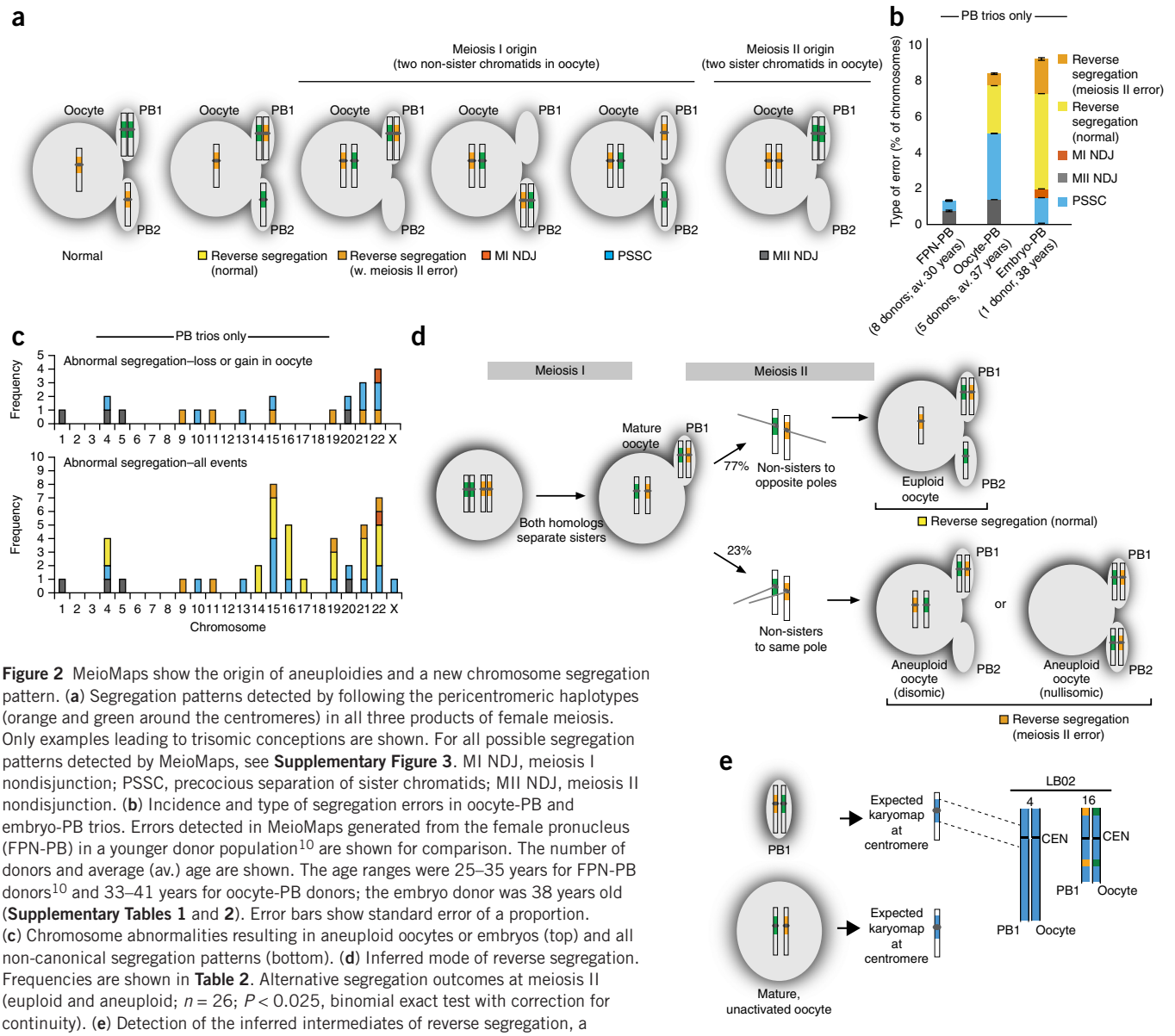

Figure 2 MeioMaps show the origin of aneuploidies and a new chromosome segregation pattern. (**a**) Segregation patterns detected by following the pericentromeric haplotypes (orange and green around the centromeres) in all three products of female meiosis. Only examples leading to trisomic conceptions are shown. For all possible segregation patterns detected by MeioMaps, see **Supplementary Figure 3**. MI NDJ, meiosis I nondisjunction; PSSC, precocious separation of sister chromatids; MII NDJ, meiosis II nondisjunction. (**b**) Incidence and type of segregation errors in oocyte-PB and embryo-PB trios. Errors detected in MeioMaps generated from the female pronucleus (FPN-PB) in a younger donor population[10] are shown for comparison. The number of donors and average (av.) age are shown. The age ranges were 25–35 years for FPN-PB donors[10] and 33–41 years for oocyte-PB donors; the embryo donor was 38 years old (**Supplementary Tables 1** and **2**). Error bars show standard error of a proportion. (**c**) Chromosome abnormalities resulting in aneuploid oocytes or embryos (top) and all non-canonical segregation patterns (bottom). (**d**) Inferred mode of reverse segregation. Frequencies are shown in **Table 2**. Alternative segregation outcomes at meiosis II (euploid and aneuploid; $n = 26$; $P < 0.025$, binomial exact test with correction for continuity). (**e**) Detection of the inferred intermediates of reverse segregation, a mature oocyte and a PB1 each containing two non-sister chromatids. The expected chromosome fingerprints corresponding to heterozygous SNPs around the centromere (CEN) are shown in blue. Two examples were found in this egg (chromosomes 4 and 16; **Table 2**).

Unexpectedly, the most frequent non-canonical segregation pattern gave rise to a PB1 that contained 2 non-sister chromatids (green and orange fingerprints around the centromeres; $n = 26$). In 20 of the 26 instances, both the oocyte and the PB2 contained normal chromosome content but had non-sister chromatids instead of sister chromatids (**Fig. 2a**). This pattern cannot be detected by the copy number analysis used previously[20], as the complement of chromosomes in the three cells is normal. We refer to this new pattern as reverse segregation, as we infer that sister chromatids of both homologs separated first in meiosis I, followed by the separation of non-sister chromatids in meiosis II (**Fig. 2d**). The equational division at meiosis I is unlikely to be the result of two independent PSSC events because the observed frequency of both homologs separating their sister chromatids is more than 100× greater than the predicted frequency for two independent PSSC events ($P < 0.001$). Consistent with equational divisions of both homologs of the chromosome at meiosis I, we observed the predicted intermediates of reverse segregation, a mature oocyte and a PB1 that contained two non-sister chromatids (**Fig. 2e** and **Table 2**). Both acrocentric and larger metacentric chromosomes displayed this reverse segregation pattern (**Fig. 2c** and **Table 2**), which was observed in all donors, ruling out the possibility that it was specific to certain women (**Supplementary Table 5**). In the remaining six cases, the two non-sister chromatids missegregated into the egg or the PB2, resulting in an aneuploid oocyte (**Fig. 2a**, reverse segregation with meiosis II error; **Supplementary Fig. 3d**). In summary, we have observed a new segregation pattern where both homologs of a chromosome undergo

Table 2 Incidence of reverse segregation

Sample type	Incidence	Chromosomes involved
Oocyte-PB1 duos (not activated)[a]	8.7 ± 4.2% ($n = 46$)	4, 13, 14, 16
Oocyte-PB1-PB2 trios	3.7 ± 1.1% ($n = 299$)	4, 11, 14, 15, 16, 19, 22
Embryo-PB1-PB2 trios	7.2 ± 1.8% ($n = 207$)	4, 9, 16, 17, 19, 21, 22

[a]See **Figure 2e**. Reverse segregation was observed in all donors (**Supplementary Table 5**).

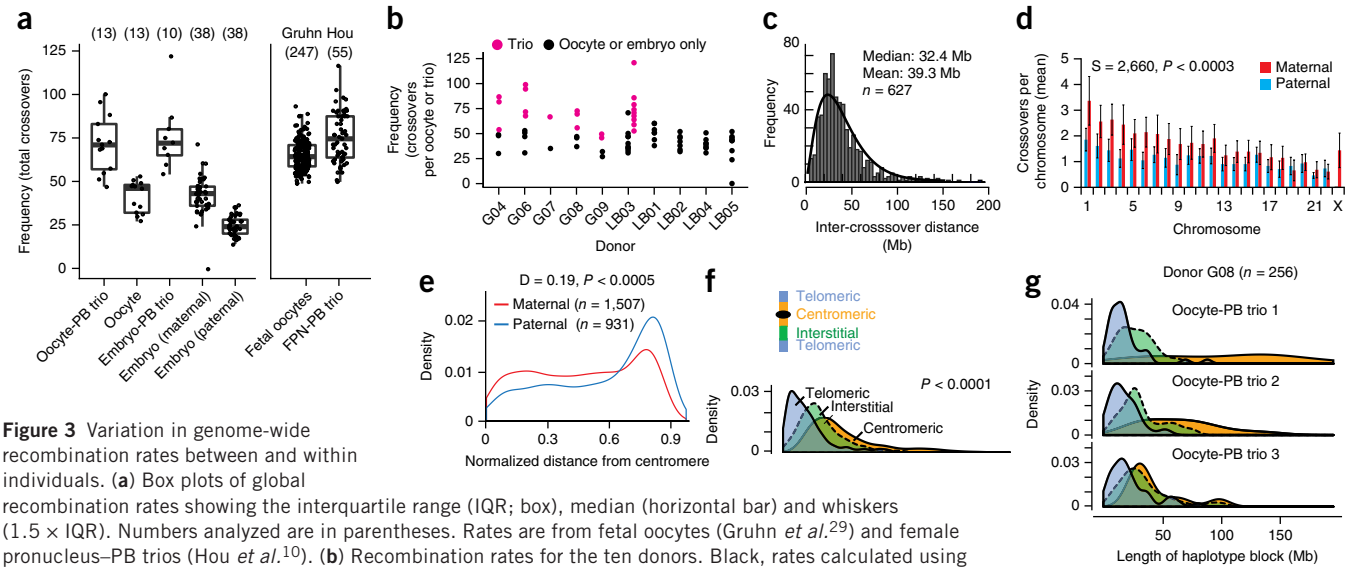

Figure 3 Variation in genome-wide recombination rates between and within individuals. (**a**) Box plots of global recombination rates showing the interquartile range (IQR; box), median (horizontal bar) and whiskers (1.5 × IQR). Numbers analyzed are in parentheses. Rates are from fetal oocytes (Gruhn *et al.*[29]) and female pronucleus–PB trios (Hou *et al.*[10]). (**b**) Recombination rates for the ten donors. Black, rates calculated using information from only the oocyte or embryo; magenta, rates calculated using information from the complete oocyte-PB trio and embryo-PB trios. (**c**) Inter-crossover distances, excluding centromeric distances. The fitted curve is based on maximum-likelihood estimation of the gamma distribution; shape, 2.6141 ± 0.14 (standard error); rate, 0.066 ± 0.0039 (standard error). Estimated fitted mean, 39.3 Mb; log-likelihood of fitting, –2,802.738; Aikaike information criterion (AIC), 5,609.476. (**d**) Average (s.d.) of chromosome-specific recombination (**Supplementary Table 3**). Generalized linear model (GLM) analysis showed that chromosome size had a significant effect on sex-specific recombination frequencies. The Spearman correlation test (S) was used to calculate the *P* values for individual pairwise comparisons between maternal and paternal recombination frequencies per chromosome. As chromosome size decreases, the contribution of sex to crossover frequencies decreases. (**e**) Crossover position relative to centromeres, normalized to chromosome length. Statistics: two-sided Kolmogorov-Smirnov test (D) of normalized and absolute lengths, $P < 0.0005$, X chromosome excluded; **Supplementary Fig. 5**). (**f**) Length of haplotype blocks (not inter-crossover distances), according to position relative to telomeric (blue), centromeric (orange) or interstitial (green) regions. Statistics: non-parametric ANOVA, $P < 0.0001$. Centromeric blocks excluded the ~3×10^6 bp of α-satellite DNA. (**g**) Variation in centromere repression of crossovers in oocyte-PB trios from the same donor.

an equational division at meiosis I, followed by a weak preference for accurate disjunction of the two non-sister chromatids at meiosis II. This pattern is reminiscent of 'inverted meiosis' in organisms with holocentric chromosomes[21–23].

Variation in global recombination rates in adult oocytes

Variation in recombination in fetal oocytes has been hypothesized to give rise to vulnerable crossover configurations that predispose chromosome pairs to missegregation decades later in adult oocytes. To assess recombination in adult oocytes and embryos, we mapped 883 maternal crossovers in the oocyte-PB trios and 1,149 and 1,342 maternal and paternal crossovers, respectively, in the embryos (**Fig. 3a** and **Supplementary Tables 5–9**). Of the reciprocal crossover events, 12% mapped to non-sister chromatids in the PB2 and oocyte, within regions of heterozygosity in the PB1. A similar proportion of events would be expected to be present in the PB1 but are undetectable because the two DNA strands cannot currently be separated and phased individually[10]. Using SNP arrays with ~300,000 markers gave median resolutions of 107 kb and 331 kb for crossovers in the oocyte-PB and embryo, respectively (**Fig. 1e**). This resolution is similar to that in high-resolution population-based studies employing SNP arrays[24–26].

Several observations support the conclusion that recombination rates in adult oocytes and embryos are highly variable, like those seen in unselected fetal oocytes[27–29]. At the same time, the average recombination frequencies are reminiscent of those reported for human populations. The average number of maternal crossovers in each oocyte or embryo was 41.6 ± 11.3 (s.d.) ($n = 51$; **Supplementary Tables 5–9**). This rate is consistent with estimates from fetal oocytes and population-based assessments[10,24,26,30–36] and with rates detected in the female pronucleus (42.5 ± 9.0 (s.d.); $n = 52$)[10]. The frequencies of the crossovers detected in the egg correlated well with those detected in the PB1 or PB2 (**Supplementary Fig. 4**). The maternal recombination rates and lengths of haplotype blocks were highly variable between donors as well as within donors[27,28,35,37], varying by as much as twofold (**Fig. 3b**,**f**,**g** and **Supplementary Fig. 4**). Using the oocyte-PB trios, maternal crossovers displayed a median distance of 32.4 Mb (**Fig. 3c**), which was in excess of the 18.3 Mb predicted by random distribution of crossovers along chromosomes (Online Methods). This finding is consistent with crossover interference along homolog pairs[10].

Embryos contain informative markers of both maternal and paternal origin. This allowed us to assess recombination of both sexes in unselected embryos for the first time. Maternal recombination rates were 1.63-fold higher than paternal rates in the embryos, consistent with population-based studies and molecular approaches on single sperm and fetal oocytes[26–32]. The additional maternal recombination events derive in part from female-only recombination along the X chromosome and in part from higher crossover frequencies on larger autosomes (**Fig. 3d**). Maternal recombination events were more centromeric than paternal events (**Fig. 3e** and **Supplementary Fig. 5**), although centromeres tended to suppress nearby recombination[10,26–32] (**Fig. 3f**). However, the suppression of centromeric crossovers varied among oocyte-PB trios, even across oocytes from the same woman (**Fig. 3g**). This variation may predispose some oocytes to crossovers positioned too close to the centromeres, which may interfere with segregation. Collectively, these observations show that the variation in total crossover numbers detected in adult oocytes is analogous to the variation in MLH1 counts observed in fetal oocytes[27–29], suggesting that MLH1 foci serve as a good proxy for crossover recombination events in human oocytes. Simultaneously, the average recombination rates are reminiscent of those in the human population.

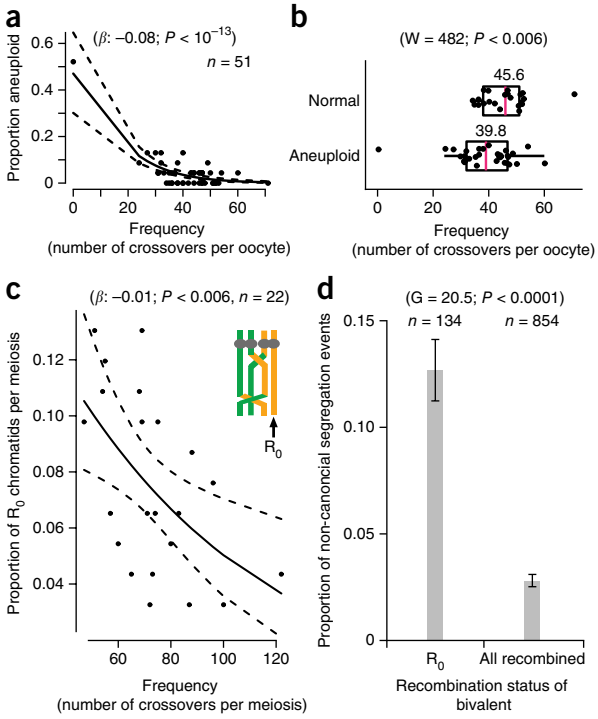

Figure 4 Higher global recombination rates protect against aneuploidy and are selected for in the human female germ line. (**a**) Logistic regression of the frequency of aneuploid chromosomes as a function of global recombination rate in the embryo or oocyte. Black lines show the logistic regression model and 95% confidence interval (dashed lines; binomial family). When the outlier with no recombination events was omitted, the regression coefficient β was –0.06 and was still highly significant ($P < 0.003$). The outlier was omitted from all subsequent statistical analyses. (**b**) Recombination rates in normal versus aneuploid oocytes and embryos. The arithmetic mean is shown above the median (magenta vertical bar). Statistics: Mann-Whitney-Wilcoxon test (W), one-sided. (**c**) Incidence of bivalents containing at least one non-recombinant (R_0) chromatid as a function of global recombination rates in oocyte-PB and embryo-PB trios. Statistics are as in **a**. (**d**) Segregation errors among chromosomes that contained one or more R_0 chromatids or where all four chromatids recombined. *P* values derived from a G test of heterogeneity (two-sided) are shown. Error bars, standard errors of a proportion ($\sqrt{(p \times (1 - p)/n)}$).

This validates our approach and lends support to the hypothesis that the variability in the rates and distribution of recombination events between and within individuals gives rise to vulnerable crossover configurations in fetal oocytes that are propagated to adult oocytes and, ultimately, embryos.

Global recombination rates as a risk factor for aneuploidy

To understand how the variability in maternal recombination rates affects human aneuploidy, we addressed whether the global, genome-wide recombination rates were correlated with the incidence of aneuploidy in individual oocytes and embryos. Indeed, global recombination rate was a strong predictor of aneuploidy (**Fig. 4a**), even when we excluded an outlier embryo that contained 12 aneuploidies and no detectable crossovers among any of the chromosome pairs. The recombination rate is an important factor, accounting for 18% of the variation in the incidence of aneuploidy (outlier excluded; permutation test).

If lower global recombination rates predispose oocytes to meiotic chromosome segregation errors, then normal euploid embryos should contain chromosomes that exhibit higher maternal genome-wide recombination frequencies than those of aneuploid embryos. To examine whether this was the case, we divided the embryos and oocytes into two groups (euploid or aneuploid) and determined their respective recombination rates (**Fig. 4b**). Normal, euploid oocytes and embryos had on average 5.8 recombination events more than aneuploid ones. This difference was significant, even when we accounted for crossovers that might not be detected owing to the presence of two chromosomes in the aneuploid oocyte[10]. Notably, the overlap in the distributions of recombination rates for the euploid and aneuploid groups is consistent with the presence of other factors that influence the fidelity of chromosome segregation[1]. Our findings suggest that higher global recombination frequencies, which are determined during fetal development, protect against errors in chromosome segregation decades later in adult woman. When errors do occur, they give rise to aneuploidy events, many of which are selected against before implantation of the embryo[38]. One implication of this is that recombination rates may be under selection in women as they enter their thirties, increasing rates by as much as 14% in women of advanced maternal age (5.8/41.5, the overall average).

Non-recombinant chromatids are at risk of PSSC

How do global recombination rates affect the segregation outcomes of individual homolog pairs? We hypothesized that lower global recombination rates might increase the risk of generating vulnerable crossover configurations. We first considered non-exchange E_0 homolog pairs, which would give rise to trios where the PB1 contains one non-recombinant homolog (green or orange) and the oocyte and PB2 contain one sister chromatid each from the other homolog if chromosome segregation is normal (**Supplementary Fig. 6a**). For the 506 chromosome pairs where crossovers could be unambiguously mapped, no such example was observed in our data, although one case was observed by Hou *et al.* (Y. Hou, personal communication). E_0 homologs may be extremely rare, or another possibility is that they missegregate. This would make inferences about the nature of the non-exchange status uncertain or putative at best. We observed 13 putative E_0 homologs among the 506 chromosome pairs across the 23 trios (**Supplementary Fig. 6d–g**). The overall incidence of these homologs (2.6%, $n = 506$) and the over-representation of the 2 smallest chromosomes (21 and 22) among those affected are reminiscent of observations of cytological markers for crossovers on fetal chromosomes in meiotic prophase[27–29]. The observed incidence of presumed E_0 homologs was much lower than expected if crossovers were randomly distributed among chromosomes (**Supplementary Fig. 6h**), which is suggestive of crossover assurance mechanism(s) in human oocytes. None of the presumed E_0 homologs followed a classical meiotic segregation pattern. Instead, they all underwent PSSC or reverse segregation (with or without meiosis II missegregation; **Supplementary Fig. 6**). This finding is consistent with the biorientation of sister chromatids of univalent chromosomes at meiosis I in model organisms[39,40].

Informative SNPs in heterozygous regions on missegregated chromosomes cannot be phased, making crossovers undetectable (**Supplementary Fig. 6**). However, most of the presumed E_0 homologs contained non-recombinant (R_0) chromatids. **Figure 4c** shows that global recombination rates are important for determining the generation of R_0 chromatids, which in turn are at increased risk of missegregation in comparison to fully recombinant bivalents (where all four chromatids engage in recombination; **Fig. 4d**). Bivalents that contained an R_0 chromatid were preferentially involved in PSSC, suggesting that non-recombinant chromatids are at risk of precociously

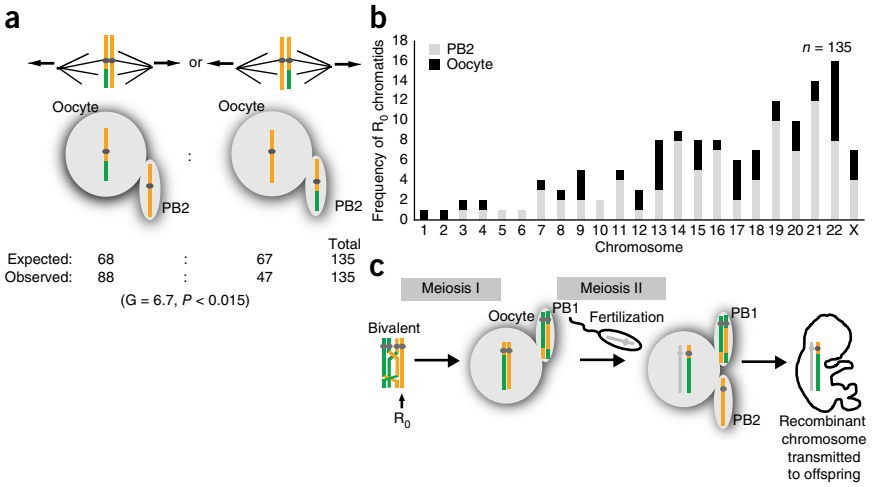

Figure 5 Meiotic drive for recombinant chromatids at meiosis II increases recombination rates in the human female germ line. (**a**) Sister chromatids are expected to segregate randomly at meiosis II. However, when chromosomes contained one non-recombinant chromatid and one recombinant chromatid, the recombinant chromatid was twice as likely to segregate to the oocyte. Statistics: G test for proportions (two-sided). (**b**) Chromosome-specific frequencies of R_0 chromatids segregating to the PB2 or oocyte. (**c**) Diagrammatic representation of meiotic drive against non-recombinant chromatids at meiosis II in the human female germ line. The paternal chromosome is shown in gray.

separating from their sister chromatid at meiosis I. It is possible that non-recombinant chromatids are at elevated risk of becoming dissociated from the rest of the bivalent during the decades-long dictyate arrest[41,42]. We conclude that recombination affects not only the generation and segregation of putative non-exchange homolog pairs but also influences the dynamics of sister chromatid segregation.

Meiotic drive for recombinant chromatids at meiosis II

Non-recombinant chromatids are not only at risk of PSSC, but their segregation at meiosis II is also affected by the lack of recombination. The MeioMaps showed 135 chromatids in an oocyte or PB2 that were non-recombinant and had segregated normally (**Fig. 5a**). These R_0 chromatids are expected to be randomly distributed among the oocyte and the PB2. Contrary to this expectation, R_0 chromatids were nearly twice as likely to be found in the PB2 than in the oocyte. The selection appears to be against non-recombinant chromatids as, when both sister chromatids recombined, their segregation was random and the recombination rates were similar in the oocyte and PB2 (**Supplementary Table 5**). We infer that, when the two sister chromatids segregated at meiosis II, non-recombinant chromatids were preferentially driven into the PB2 and thus eliminated from the human germ line (**Fig. 5b**,**c**). The use of asymmetric cell divisions during oogenesis for the preferential inclusion of an allele[43] or even whole chromosomes[44–46] is referred to as meiotic or chromosomal drive. The meiotic drive against non-recombinant chromatids resulted in a 6.6% elevation in the recombination rates in oocytes as compared to the PB2 (**Supplementary Table 5**). These findings imply that recombination is not only important for the accurate segregation of homologs at meiosis I but also acts as a driving force during sister chromatid segregation at meiosis II. Selection against non-recombinant chromatids may prevent entire chromosomes from being inherited as a single haplotype block, thereby reducing the probability of inbreeding or propagation of segregation distorters[47–49]. This may be meaningful both in terms of population structure and the genomic health of children. The difference in genome structure between the PB2 and oocyte is particularly relevant because the PB2 has been proposed for use in treatment of mitochondrial disease[50].

DISCUSSION

Until recently, recombination and chromosome segregation were studied in populations, where polar body information was not available, or in fetal oocytes, which arise decades before the segregation events being studied. MeioMaps from unselected adult oocytes, the female pronucleus in zygotes[10] and embryos now provide a 'missing link' between events that occur during fetal development and their influence on chromosome segregation outcomes decades later in the adult oocyte.

Recombination rates in unselected oocytes were 1.6-fold higher than in males and showed a broad distribution, similar to the high degree of variation in fetal oocytes[27–29]. Sex-specific differences in chromosome structure during meiotic prophase have been suggested to explain this difference, with female chromosomes having a longer axis and shorter chromatin loops[51]. Increased loop number correlates with the increased recombination rate in female meiosis[29,51]. Although the mean female recombination rates were similar to those seen in populations, the range was substantially broader. We found that lower genome-wide recombination rates were selected against because they were less likely to give rise to a euploid oocyte. This is consistent with findings that individuals with Down syndrome have lower genome-wide recombination rates than their euploid siblings[25]. This degree of selection is not observed in younger women[10] and could contribute to the higher recombination rates in children as mothers age[24,32,52]. This model predicts that children born to younger mothers should display a broader range in recombination frequencies than those born to women of advanced maternal age.

Lower genome-wide recombination rates increase the risk of at least two types of vulnerable crossover configurations: non-recombinant (R_0) chromatids and putative non-exchange (E_0) homologs. Non-recombinant (R_0) chromatids are a risk factor for PSSC and show preferential segregation to the PB2 at meiosis II (meiotic drive). Putative E_0 homologs underwent either PSSC or a new reverse segregation pattern, where sister chromatids of both homologs separated at meiosis I, followed by a weak preference for accurate division of the two non-sister chromatids at meiosis II. The reverse segregation pattern is not limited to E_0 homologs and could be the result of centromeric crossovers that fall at or within 1–2 Mb of the centromere, the positions of the last informative SNPs (**Supplementary Table 10**). Centromeric crossovers interfere with segregation of sister chromatids in *Drosophila melanogaster*[7] and budding yeast[8] and are associated with an increased risk of aneuploidy in humans[1]. The relatively high incidence of meiosis II nondisjunction (23%, $n = 26$) associated with reverse segregation could be explained by crossover in the extreme vicinity of centromeres. Another possible mechanism that seems particularly plausible for the larger metacentric chromosomes, where two crossovers would have to occur within 1 Mb on both sides of the centromere, is that homologs segregate their

sister chromatids in an equational fashion in meiosis I, followed by a weak preference for accurate non-sister chromatid segregation at meiosis II (77% compared to 50% expected by random chance, $n = 26$; $P < 0.05$). It is possible that failure to establish crossovers or maintain the bivalent structure during the extended dictyate arrest might predispose to equational division at meiosis I. This could occur by deterioration of cohesion between sister chromatids or sister kinetochores or by bivalents falling apart into univalents. There is evidence for the latter in human meiosis I oocytes[53,54], but it is unknown whether the frequencies and chromosome-specific effects of such events match the maternally derived, age-related component underlying human aneuploidies. In mouse oocytes, univalents preferentially segregate sister chromatids at meiosis I (refs. 39,40), and this may also be the case in humans. At meiosis II, non-sister chromatids could be physically attached by unresolved recombination intermediates (joint molecules)[55] or other threads[21,22,56], or the oocyte may use segregation mechanisms that do not rely on physical attachment between chromosomes[57]. The relative contributions of reverse segregation mechanisms and centromeric crossovers remain to be determined but in either case demonstrate that events attributed to mistakes in chromosome segregation in meiosis II can have their origin at meiosis I in human female meiosis.

METHODS

Methods and any associated references are available in the online version of the paper.

Note: Any Supplementary Information and Source Data files are available in the online version of the paper.

ACKNOWLEDGMENTS

We gratefully acknowledge C. May, A. Eyre-Walker, J. Gruhn, R. Rowsey, J. Turner, F. Cole and members of the Hoffmann laboratory for discussion and critical reading of the manuscript. We thank Y. Hou, W. Fan and S. Xie for freely sharing data and discussion on their study of female pronucleus–PB trios. Financial support for this research was provided by the UK Medical Research Council (Senior Research Fellowship to E.R.H.; G0902043) and a European Molecular Biology Organization (EMBO) Young Investigator award to E.R.H.

AUTHOR CONTRIBUTIONS

A.C., C.S.O., D.C., L.R., F.M.U., K.S., M.C.S. and A.R.T. were responsible for donor consenting, oocyte collection and oocyte activation. L.R., F.M.U., A.H.H. and K.S. oversaw ethical and legal regulation in Italy and the UK. A.C., C.S.O., S.A.N., H.A.J. and D.C. carried out amplification, SNP array and aCGH experiments. A.H.H., L.J.N., C.S.O. and E.R.H. analyzed the encoded data. E.R.H. and A.D.H. carried out data analysis and simulations. E.R.H. and E.H. carried out statistical analyses. E.R.H., A.H.H. and L.J.N. generated the figures. E.R.H., A.H.H., L.J.N. and C.S.O. wrote the manuscript. A.H.H., C.S.O., D.K.G., A.C., L.J.N. and E.R.H. edited the manuscript. All authors proofread and accepted the manuscript.

COMPETING FINANCIAL INTERESTS

The authors declare no competing financial interests.

1. Nagaoka, S.I., Hassold, T.J. & Hunt, P.A. Human aneuploidy: mechanisms and new insights into an age-old problem. *Nat. Rev. Genet.* **13**, 493–504 (2012).
2. Hassold, T. & Hunt, P. To err (meiotically) is human: the genesis of human aneuploidy. *Nat. Rev. Genet.* **2**, 280–291 (2001).
3. Zaragoza, M.V. *et al.* Nondisjunction of human acrocentric chromosomes: studies of 432 trisomic fetuses and liveborns. *Hum. Genet.* **94**, 411–417 (1994).
4. Hassold, T.J. & Jacobs, P.A. Trisomy in man. *Annu. Rev. Genet.* **18**, 69–97 (1984).
5. Hassold, T. *et al.* A cytogenetic study of 1000 spontaneous abortions. *Ann. Hum. Genet.* **44**, 151–178 (1980).
6. Freeman, S.B. *et al.* The National Down Syndrome Project: design and implementation. *Public Health Rep.* **122**, 62–72 (2007).
7. Koehler, K.E. *et al.* Spontaneous X chromosome MI and MII nondisjunction events in *Drosophila melanogaster* oocytes have different recombinational histories. *Nat. Genet.* **14**, 406–414 (1996).
8. Rockmill, B., Voelkel-Meiman, K. & Roeder, G.S. Centromere-proximal crossovers are associated with precocious separation of sister chromatids during meiosis in *Saccharomyces cerevisiae*. *Genetics* **174**, 1745–1754 (2006).
9. Hultén, M.A., Patel, S., Jonasson, J. & Iwarsson, E. On the origin of the maternal age effect in trisomy 21 Down syndrome: the oocyte mosaicism selection model. *Reproduction* **139**, 1–9 (2010).
10. Hou, Y. *et al.* Genome analyses of single human oocytes. *Cell* **155**, 1492–1506 (2013).
11. Handyside, A.H. *et al.* Karyomapping: a universal method for genome wide analysis of genetic disease based on mapping crossovers between parental haplotypes. *J. Med. Genet.* **47**, 651–658 (2010).
12. Natesan, S.A. *et al.* Genome-wide karyomapping accurately identifies the inheritance of single-gene defects in human preimplantation embryos *in vitro*. *Genet. Med.* **16**, 838–845 (2014).
13. Alfarawati, S. *et al.* The relationship between blastocyst morphology, chromosomal abnormality, and embryo gender. *Fertil. Steril.* **95**, 520–524 (2011).
14. Kuliev, A., Zlatopolsky, Z., Kirillova, I., Spivakova, J. & Cieslak Janzen, J. Meiosis errors in over 20,000 oocytes studied in the practice of preimplantation aneuploidy testing. *Reprod. Biomed. Online* **22**, 2–8 (2011).
15. Gutiérrez-Mateo, C. *et al.* Validation of microarray comparative genomic hybridization for comprehensive chromosome analysis of embryos. *Fertil. Steril.* **95**, 953–958 (2011).
16. Capalbo, A. *et al.* Sequential comprehensive chromosome analysis on polar bodies, blastomeres and trophoblast: insights into female meiotic errors and chromosomal segregation in the preimplantation window of embryo development. *Hum. Reprod.* **28**, 509–518 (2013).
17. Franasiak, J.M. *et al.* The nature of aneuploidy with increasing age of the female partner: a review of 15,169 consecutive trophectoderm biopsies evaluated with comprehensive chromosomal screening. *Fertil. Steril.* **101**, 656–663 (2014).
18. Reiger, R., Michaelis, A. & Green, M.M. *Glossary of Genetics and Cytogenetics* (Springer Verlag, 1968).
19. Angell, R.R. Predivision in human oocytes at meiosis I: a mechanism for trisomy formation in man. *Hum. Genet.* **86**, 383–387 (1991).
20. Handyside, A.H. *et al.* Multiple meiotic errors caused by predivision of chromatids in women of advanced maternal age undergoing *in vitro* fertilisation. *Eur. J. Hum. Genet.* **20**, 742–747 (2012).
21. Heckmann, S. *et al.* Alternative meiotic chromatid segregation in the holocentric plant *Luzula elegans*. *Nat. Commun.* **5**, 4979 (2014).
22. Cabral, G., Marques, A., Schubert, V., Pedrosa-Harand, A. & Schlogelhofer, P. Chiasmatic and achiasmatic inverted meiosis of plants with holocentric chromosomes. *Nat. Commun.* **5**, 5070 (2014).
23. Viera, A., Page, J. & Rufas, J.S. Inverted meiosis: the true bugs as a model to study. *Genome Dyn.* **5**, 137–156 (2009).
24. Coop, G., Wen, X., Ober, C., Pritchard, J.K. & Przeworski, M. High-resolution mapping of crossovers reveals extensive variation in fine-scale recombination patterns among humans. *Science* **319**, 1395–1398 (2008).
25. Middlebrooks, C.D. *et al.* Evidence for dysregulation of genome-wide recombination in oocytes with nondisjoined chromosomes 21. *Hum. Mol. Genet.* **23**, 408–417 (2014).
26. Kong, A. *et al.* A high-resolution recombination map of the human genome. *Nat. Genet.* **31**, 241–247 (2002).
27. Lenzi, M.L. *et al.* Extreme heterogeneity in the molecular events leading to the establishment of chiasmata during meiosis I in human oocytes. *Am. J. Hum. Genet.* **76**, 112–127 (2005).
28. Cheng, E.Y. *et al.* Meiotic recombination in human oocytes. *PLoS Genet.* **5**, e1000661 (2009).
29. Gruhn, J.R., Rubio, C., Broman, K.W., Hunt, P.A. & Hassold, T. Cytological studies of human meiosis: sex-specific differences in recombination originate at, or prior to, establishment of double-strand breaks. *PLoS ONE* **8**, e85075 (2013).
30. Broman, K.W., Murray, J.C., Sheffield, V.C., White, R.L. & Weber, J.L. Comprehensive human genetic maps: individual and sex-specific variation in recombination. *Am. J. Hum. Genet.* **63**, 861–869 (1998).
31. Tease, C., Hartshorne, G.M. & Hulten, M.A. Patterns of meiotic recombination in human fetal oocytes. *Am. J. Hum. Genet.* **70**, 1469–1479 (2002).
32. Kong, A. *et al.* Recombination rate and reproductive success in humans. *Nat. Genet.* **36**, 1203–1206 (2004).
33. Myers, S., Bottolo, L., Freeman, C., McVean, G. & Donnelly, P. A fine-scale map of recombination rates and hotspots across the human genome. *Science* **310**, 321–324 (2005).
34. Kong, A. *et al.* Sequence variants in the *RNF212* gene associate with genome-wide recombination rate. *Science* **319**, 1398–1401 (2008).
35. Kong, A. *et al.* Fine-scale recombination rate differences between sexes, populations and individuals. *Nature* **467**, 1099–1103 (2010).
36. Kong, A. *et al.* Common and low-frequency variants associated with genome-wide recombination rate. *Nat. Genet.* **46**, 11–16 (2014).
37. Chowdhury, R., Bois, P.R., Feingold, E., Sherman, S.L. & Cheung, V.G. Genetic analysis of variation in human meiotic recombination. *PLoS Genet.* **5**, e1000648 (2009).
38. Capalbo, A. *et al.* Correlation between standard blastocyst morphology, euploidy and implantation: an observational study in two centers involving 956 screened blastocysts. *Hum. Reprod.* **29**, 1173–1181 (2014).
39. LeMaire-Adkins, R. & Hunt, P.A. Nonrandom segregation of the mouse univalent X chromosome: evidence of spindle-mediated meiotic drive. *Genetics* **156**, 775–783 (2000).

40. Kouznetsova, A., Lister, L., Nordenskjold, M., Herbert, M. & Hoog, C. Bi-orientation of achiasmatic chromosomes in meiosis I oocytes contributes to aneuploidy in mice. *Nat. Genet.* **39**, 966–968 (2007).
41. Wolstenholme, J. & Angell, R.R. Maternal age and trisomy—a unifying mechanism of formation. *Chromosoma* **109**, 435–438 (2000).
42. Garcia-Cruz, R. *et al.* Dynamics of cohesin proteins REC8, STAG3, SMC1β and SMC3 are consistent with a role in sister chromatid cohesion during meiosis in human oocytes. *Hum. Reprod.* **25**, 2316–2327 (2010).
43. Sandler, L. & Novitski, E. Meiotic drive as an evolutionary force. *Am. Nat.* **91**, 105–110 (1957).
44. Bongiorni, S., Fiorenzo, P., Pippoletti, D. & Prantera, G. Inverted meiosis and meiotic drive in mealybugs. *Chromosoma* **112**, 331–341 (2004).
45. Pardo-Manuel de Villena, F. & Sapienza, C. Nonrandom segregation during meiosis: the unfairness of females. *Mamm. Genome* **12**, 331–339 (2001).
46. Dawe, R.K. & Cande, W.Z. Induction of centromeric activity in maize by *suppressor of meiotic drive 1*. *Proc. Natl. Acad. Sci. USA* **93**, 8512–8517 (1996).
47. Haig, D. & Grafen, A. Genetic scrambling as a defence against meiotic drive. *J. Theor. Biol.* **153**, 531–558 (1991).
48. Chmátal, L. *et al.* Centromere strength provides the cell biological basis for meiotic drive and karyotype evolution in mice. *Curr. Biol.* **24**, 2295–2300 (2014).
49. Brandvain, Y. & Coop, G. Scrambling eggs: meiotic drive and the evolution of female recombination rates. *Genetics* **190**, 709–723 (2012).
50. Wang, T. *et al.* Polar body genome transfer for preventing the transmission of inherited mitochondrial diseases. *Cell* **157**, 1591–1604 (2014).
51. Lynn, A. *et al.* Covariation of synaptonemal complex length and mammalian meiotic exchange rates. *Science* **296**, 2222–2225 (2002).
52. Campbell, C.L., Furlotte, N.A., Eriksson, N., Hinds, D. & Auton, A. Escape from crossover interference increases with maternal age. *Nat. Commun.* **6**, 6260 (2015).
53. Angell, R. First-meiotic-division nondisjunction in human oocytes. *Am. J. Hum. Genet.* **61**, 23–32 (1997).
54. Garcia-Cruz, R. *et al.* Cytogenetic analyses of human oocytes provide new data on non-disjunction mechanisms and the origin of trisomy 16. *Hum. Reprod.* **25**, 179–191 (2010).
55. Copsey, A. *et al.* Smc5/6 coordinates formation and resolution of joint molecules with chromosome morphology to ensure meiotic divisions. *PLoS Genet.* **9**, e1004071 (2013).
56. Hughes, S.E. *et al.* Heterochromatic threads connect oscillating chromosomes during prometaphase I in *Drosophila* oocytes. *PLoS Genet.* **5**, e1000348 (2009).
57. Hughes-Schrader, S. Distance segregation and compound sex chromosomes in mantispids (Neuroptera:Mantispidae). *Chromosoma* **27**, 109–129 (1969).

ONLINE METHODS

Ethics statement. All material for the study was ethically sourced with fully informed patient consent. All oocytes for the study were obtained from donors after completion of their IVF treatment and were destroyed for analysis. The oocytes used were vitrified in accordance with Italian law in place at the time of oocyte retrieval for IVF treatment. Use of the oocytes for the study was approved by the Institutional Review Board of the Valle Giulia Clinic where the oocytes were stored and did not influence patient treatment. All embryo samples for the study were either obtained by tubing embryos in their entirety (destroyed) for analysis following a previous abnormal outcome in clinical tests or reanalysis of clinical biopsy samples after embryos were transferred, stored or discarded, depending on the clinical result. SNP genotyping was performed as clinical follow-up or validation of clinical genetic analysis and was covered by the Human Fertilisation and Embryology Authority (HFEA) code of practice. All primary data were encoded such that informative SNPs were represented as A and B. Only secondary data with informative SNPs coded as A and B were used for data analysis.

Oocyte–polar body trios. *Patient participation and consent.* All meiosis II oocytes for the study were obtained from patients undergoing ICSI treatment in the Centre for Reproductive Medicine GENERA in Rome between 2 September 2008 and 15 May 2009 following controlled ovarian hyperstimulation performed using two different protocols: the gonadotropin-releasing hormone (GnRH)-agonist long protocol and the GnRH-antagonist protocol. According to Italian law in force when these oocytes were collected, a maximum of three oocytes could be inseminated per patient. The remaining meiosis II oocytes were vitrified and later included in the study after informed consent was obtained from the patients. The study and informed consent were approved by the Institutional Review Board of the Valle Giulia Clinic and did not influence patient treatment.

Oocyte collection. Oocyte collection was performed 35 h after the administration of human chorionic gonadotropin (hCG). Removal of the cumulus mass was performed by brief exposure to 40 IU/ml hyaluronidase solution in Sage fertilization medium supplemented with 10% human serum albumin (HSA; Cooper Surgical), followed by mechanical removal of the corona radiata with the use of plastic 'denuding' pipettes of defined diameters (COOK Medical) in a controlled 6% CO_2 and 37 °C environment. This procedure was performed between 37 and 40 h after administration of hCG. Meiosis II oocytes were then identified for vitrification.

Oocyte vitrification and warming. The vitrification and warming procedures were performed as described by Kuwayama *et al.*[58,59]. Commercially available vitrification and warming kits were used (Kitazato BioPharma). The vitrification procedure was performed a maximum of 40 h after administration of hCG. Oocytes were stored on a cryotop vitrification tool (Kitazato BioPharma) with a plastic cap for protection during storage in liquid nitrogen. All oocytes were stored submerged in liquid nitrogen until warming was performed. After oocyte warming, degenerated oocytes were discarded and the surviving oocytes were cultured before biopsy of PB1 and activation.

Oocyte culture and activation. All oocyte culture was performed at 37 °C in 6% CO_2 and 5% O_2. To enable tracking of the oocytes and PBs, individual culture was performed and culture drops and wells were numbered to allow traceability throughout the experiment.

Immediately after warming, the surviving oocytes were allocated to individually numbered 35-µl microdrops of Sage cleavage medium supplemented with 10% HSA under mineral oil (Cooper Surgical) and cultured for 2 h before PB1 biopsy and activation.

Oocytes were activated by exposure to activation medium, comprising 100 µM calcium ionophore (A23187, C7522, Sigma-Aldrich) in Sage cleavage medium supplemented with 10% HSA, from a stock solution in DMSO (Sigma-Aldrich) diluted 1:40. Oocytes were transferred to 35-µl drops of the activation medium under Sage mineral oil, numbered appropriately. Activation culture was performed for 40–120 min. The oocytes were then moved to post-activation culture.

Post-activation culture was performed in separate wells of EmbryoScope slides (Unisence Fertilitech) in cleavage medium—the medium used for culture after warming—under Sage mineral oil. Slides were placed in the EmbryoScope time-lapse incubator (Unisence Fertilitech) for assessment of PB2 extrusion and the appearance of pronuclei before PB2 biopsy.

Polar body biopsy. Polar bodies were biopsied sequentially to discriminate between the three products of meiosis, using micromanipulators (Narishige) on an inverted microscope (Nikon) equipped with Hoffman Modulation contrast and a 37 °C heating stage (Linkam Scientific Instruments). The PB1 was biopsied before oocyte activation, and the PB2 was biopsied following its extrusion after activation as previously described by Capalbo *et al.*[16]. All biopsies were performed in individually numbered 10-µl microdrops of HEPES medium supplemented with 10% HSA under Sage mineral oil for tractability. For both the PB1 and PB2 biopsies, oocytes were positioned on the microscope to give a clear view of the polar body and secured by suction with the holding pipette (TPC). An aperture was made in the zona pelucida with a series of laser pulses (Saturn Laser, Research Instruments), working inward from the outer surface of the zona pelucida. The aspiration pipette (zona pelucida–drilling pipette; TPC) was then inserted through the opening, and the polar body was removed with gentle suction. Once the PB1 was biopsied, the oocyte was moved to activation culture, leaving the biopsied PB1 in the microdrop for immediate transfer a 0.2-ml RNase- and DNase-free thin-walled, flat-cap PCR tube (Corning, Sigma-Aldrich) for DNA amplification. Once the PB2 was biopsied, it was immediately transferred to a PCR tube for DNA amplification, with the oocyte still in the microdrop. The oocyte was then returned to the micromanipulator for full zona pelucida removal. The zona pelucida was removed from each oocyte using the same setup for the biopsy procedure. The oocyte was anchored to the holding pipette, and a larger aperture was created in the zona pelucida using laser pulses. The oocyte was removed from the zona pelucida using both displacement and zona pelucida manipulation techniques with the aspiration pipette. Once free from the zona pelucida, the oocyte was transferred to a PCR tube for DNA amplification.

Transfer of the samples to PCR tubes was performed using a plastic denuding pipette with a 130-µm lumen. Individually labeled PCR tubes were primed with 2 µl of Dulbecco's PBS (DPBS, Gibco, Life Technologies) with 0.1% polyvinyl alcohol (Sigma-Aldrich). Individual samples were expelled into the DPBS in around 1 µl of the medium containing the sample, leaving a final volume of no more than 4 µl of medium with the sample in each PCR tube. The PCR tubes were then briefly centrifuged, snap frozen in liquid nitrogen and stored at −20 °C before whole-genome amplification.

DNA extraction and whole-genome amplification. Genomic DNA from all oocyte donors was obtained using buccal cell swabs (Isohelix, Cell Projects). Extraction of genomic DNA from the swabs was performed using a proteinase K extraction kit (Isohelix, Cell Projects) for a final volume of 30 µl, following the manufacturer's instructions. DNA from all three products of meiosis was obtained by lysis of the cells and whole-genome amplification. The PCR tubes containing samples were brought to a final volume of 4 µl with PBS, and REPLI-g Single-Cell kit multiple-displacement amplification (SureMDA, Illumina) or PCR library-based SurePlex amplification (Illumina) was performed according to the manufacturer's instructions. Multiple-displacement amplification was performed with a short 2-h incubation.

Embryos and embryo-PB trios. *Embryo samples.* Thirty-five embryos diagnosed as affected and/or aneuploid were analyzed from four clinical cases for either PGD of single-gene defects or PGS for aneuploidy, following standard IVF protocols at the Bridge Centre (London) with informed consent from the patients. SNP genotyping was performed for quality control purposes, following clinical biopsy and genetic testing of the embryos under HFEA clinic license L0070-14-a, using similar methods to those described for the processing of the oocyte-PB trios.

In one of the PGD cases, two surplus denuded meiosis I oocytes were allowed to mature *in vitro* by overnight culture in Sage fertilization medium supplemented with10% HSA under mineral oil. Biopsy of PB1, tubing and whole-genome amplification for the oocyte and PB1 were then performed as described for the oocyte-PB trios.

Embryo-PB trios. In another PGS case, in which aCGH had been used to detect aneuploidy by copy number analysis of both polar bodies, the whole-genome amplification products (SurePlex) from both polar bodies were SNP

doi:10.1038/ng.3306

genotyped, along with parental genomic DNA and, with informed consent from the patients, the whole-genome amplification products (SureMDA) of nine corresponding fertilized embryos that had all been diagnosed as aneuploid.

aCGH, SNP bead array and data analysis. For aCGH analysis, 4-µl aliquots of SurePlex single-cell amplified DNA products (from the PB1, PB2, and oocyte or blastomere) were processed on microarray slides (24Sure, Illumina). Data were imported and analyzed using dedicated software (BlueFuse Multi v 4.0, Illumina).

For SNP genotyping, 400 ng of genomic DNA or 8 µl of the whole-genome amplification products from the single-cell and embryo samples (PB1, PB2, and oocyte, single blastomere or whole embryo) was processed on the Human CytoSNP-12 or Human Karyomapping BeadChip array (Illumina) for ~300,000 SNPs, using a shortened protocol. The genotype data were analyzed using a dedicated software program for karyomapping (BlueFuse Multi v 4.0) or exported as a text file for analysis in Microsoft Excel[12].

MeioMap analysis. Following SNP genotyping, MeioMaps were constructed and displayed by importing the data into Excel and processing it using custom macros written in Visual Basic for Applications. For the oocyte-PB trios, a simple algorithm was applied to phase all heterozygous maternal SNP loci using a haploid PB2 or oocyte sample as the reference. This defined a reference set of homozygous SNP loci (haplotype; AA or BB) for the whole genome across each chromosome. The genotype of each of the samples, including the reference, was then interrogated at each of these informative SNP loci and displayed as the same as the reference (orange), opposite to the reference (green) or heterozygous (blue), indicating the presence of both maternal haplotypes. Phase transitions at crossovers were then manually tagged in Excel by copying the closest SNP calls bracketing each crossover, and the type and positions of these SNPs were imported into a second spreadsheet for further processing. Because phasing was achieved using a reference sample, any phase transitions caused by crossovers in that particular sample appear in identical positions in all other samples analyzed (with the exception of any crossover between the reference and the PB2 or oocyte in that trio). Macros in the second spreadsheet therefore identified these common crossovers, restored them to the reference sample and removed them from all the other samples. The MeioMaps were then displayed, checked and further edited manually as necessary. All oocyte-PB trios were run with at least two references to MeioMap any aneuploid chromosomes in the reference trio and to double-check all crossovers.

For embryo-PB trios, two methods were used. Where the SNP genotype of a close relative or, in some cases, a sibling embryo was available, the samples were karyomapped using the standard algorithm, which identifies informative SNP loci for all four parental haplotypes either in Excel or using dedicated software (BlueFuse Multi v 4.0)[11,12]. Alternatively, to improve resolution, a modified karyomapping algorithm, with a PB2 or oocyte as the reference, was used. This algorithm identified all combinations of parental genotypes that were informative for the maternal haplotype only. In either case, the phase transitions were manually tagged and imported into a second spreadsheet for further processing, display and final editing, as described above.

We validated our workflow on single cells by comparing recombination maps in 15 individual cells from a donor to the genomic DNA of the child and by assessing 10 individual blastomeres from the same embryo for direct comparison. In all cases, the concordance of recombination rates and positions was >99% (data not shown).

Simulation: crossover distribution among chromosomes and distances between crossovers along chromosomes. Twelve percent of crossovers were mapped in the PB2 and oocyte. A similar proportion would be expected to be present in the PB1, but these events are undetectable because heterozygous SNPs (blue regions) cannot be phased.

Maternal recombination rates in the oocyte-PB and embryo-PB trios were similar to those reported for fetal oocytes[27–29] as well as female pronucleus–PB trios from young women[10]. When only the embryo or oocyte was used, >50% of crossovers went undetected in the two polar bodies (**Fig. 3a**,**b**). The recombination rates in the oocyte or embryo correlated well with those discerned in the polar bodies (**Supplementary Fig. 3**). This supports the notion that recombination occurs randomly among non-sister chromatids. Indeed, when homolog pairs had engaged in crossing over twice, no evidence of an increased or decreased probability of the same two chromatids engaging in the second crossover as in the first was detected. This is consistent with reports that the preference for two sister chromatids to re-engage in a second crossover given their involvement in a first crossover (negative chromatid interference) is very weak[10].

Simulations were performed to allocate a specified number of crossover events to the set of chromosomes. Chromosomes were allocated a specified length using the minimum and maximum distances between the crossover locations mapped within the experimental data set. Crossovers were allocated randomly to chromosomes with weighted probability using the chromosome length; thus, longer chromosomes received more crossovers. Allocation was either completely random (non-obligate) or random following allocation of one crossover per chromosome (obligate). For each chromosome, the position of an allocated crossover was determined iteratively by randomly selecting an available location. The available locations included all possible positions not within the minimum distance (107 kb) from an existing crossover position. The simulation reported the total number of crossovers per chromosome and the inter-crossover distances. The distance from the outermost crossover to the chromosome terminus was not included. Ten thousand simulations were performed to create the distributions. The scripts (Ottolini_Scripts_CrossoverData.pl) are freely available under copyright and GNU public license.

To estimate the fraction of missed crossovers, we randomly distributed 125 crossovers along chromosomes with a minimum distance of 0 kb between them (Ottolini_Scripts_CrossoverData.pl). A cumulative distribution of inter-crossover distances was constructed, ignoring distances for crossover that were adjacent to telomeres. The cumulative frequencies were 0.04% at 10 kb, 0.15% at 30 kb, 0.52% at 107 kb, 0.75% at 150 kb and 1% at 200 kb.

Chromatid interference. To detect chromatid interference, we identified 134 chromosome pairs with 2 crossovers and we asked whether the same 2 chromatids were less or more likely to be involved in both crossover events as compared to random participation. We were unable to reject the null hypothesis of no chromatid interference ($P > 0.5$, t test for proportions), consistent with reports that negative chromatid interference is weak[10].

Statistics, modeling and graphics. Statistical tests and modeling were carried out in Perl or R. All tests were permutation and non-parametric tests or logistic regression analysis, as indicated throughout the manuscript. For logistic regression, we used the AIC to choose the appropriate link function. Binomial distributions of error variances were assessed using the plot(model) function in R. Residual variance and degrees of freedom were tested using χ^2 tests, and the null hypothesis was rejected if the P value was below 5%. Two-sided tests were employed, unless otherwise indicated. We used the lme4, lmPerm and psperman libraries in R. Graphics were rendered using basic functions in R or the ggplot2 library[60].

58. Kuwayama, M. Highly efficient vitrification for cryopreservation of human oocytes and embryos: the Cryotop method. *Theriogenology* **67**, 73–80 (2007).
59. Kuwayama, M., Vajta, G., Kato, O. & Leibo, S.P. Highly efficient vitrification method for cryopreservation of human oocytes. *Reprod. Biomed. Online* **11**, 300–308 (2005).
60. Wickham, H. *ggplot2: Elegant Graphics for Data Analysis* (Springer, 2009).